Enhancement of adhesion by applying amine primer to isotactic polypropylene and open time dependence of primer effect

Komada, Megumi ; Nakanishi, Yuta ; Matsumoto, Takuya ; Kotera, Masaru ; Hongo, Chizuru ; Nishino, Takashi

(Citation)
International Journal of Adhesion and Adhesives,84:173-177

(Issue Date)
2018-08

(Resource Type)
journal article

(Version)
Accepted Manuscript

Enhancement of adhesion by applying amine primer to *isotactic* polypropylene and open time dependence of primer effect

Megumi Komada[a], Yuta Nakanishi[a], Takuya Matsumoto[a], Masaru Kotera[a], Chizuru Hongo[a], and Takashi Nishino[a]*

[a] Department of Chemical Science and Engineering, Graduate School of Engineering, Kobe University, Rokko, Nada, Kobe, 657-8501, Japan

Key Word

Adhesion strength, Polypropylene, Dimethyloctadecylamine, Primer effect, X-ray diffraction, Cyanoacrylate adhesion

ABSTRACT

Primer treatments to improve the adhesive properties of *isotactic* polypropylene (*it.*PP) have advantages in terms of their simple process and reasonable costs. However, a large contribution to the optimization of the treatment condition is required because of many parameters for achieving high adhesion strength. In addition, the mechanisms of primer effects have not been explained completely. We investigated the primer effects of dimethyloctadecylamine on the *it.*PP surface from the viewpoint of structural and surface properties. The *it.*PP main chains in the thin film state were aligned in parallel to the substrates. After amine primer treatment, the dimethyloctadecylamine assembled on the *it.*PP layer within 5 h. The primer alignments enhanced adhesive strength between *it.*PP and cyanoacrylate adhesives. The surface free energy of *it.*PP and cyanoacrylate adhesives was also increased by primer treatment. The time dependence of primer effects on the adhesion strength and surface properties was clarified.

Introduction

Poly-α-olefins are the most familiar and versatile polymers in our daily life. They are widely accepted as components of food packaging, various daily necessities, electric home appliance parts, and automobile components.[1,2] This acceptance is attributed to their high mechanical properties, high thermal stability, durability against chemical reagents, immense processability and admirable cost-effectiveness. Additionally, their properties can be improved further through mixing with inorganic particles or fibers, blending with other polymers, or laminating.[2–5] The ability to control these physical properties led to increasing use of poly-α-olefins in various industries. Numerous poly-α-olefin derivatives have been reported, and among these, *isotactic* polypropylene, namely *it.*PP, has attracted considerable attention~~s~~ since Ziegler and Natta discovered catalysts for the synthesis of *it.*PP in the 1950s.[6,7] Besides its high performances in various applications, however, the critical disadvantage of *it.*PP is its poor adhesion. This is caused by its high crystallinity and the absence of a polar functional group in the chemical structure. In the case of integration between several components, this disadvantage leads to defects in the products. Therefore, surface modification of *it.*PP has been focused on.[8] Various modification methods have been proposed such as blast, flame, UV, plasma, corona discharge, chromate, and primer treatments.[9–19]

The primer treatment is one of the most simple and facile surface modification methods. The procedure involves only pasting primers on the *it.*PP substrates, which is known to improve the adhesive properties of *it.*PP. The primers include various types of polyurethane, polyethyleneimine and chlorinated polypropylene for laminating, painting and printing. Sakamoto and co-workers have reported on the primer effect of poly(stearic methacrylate-*co*-dimethylaminoethyl methacrylate).[20] Moreover, it has been reported that alkyl amines served as primers for the adhesion between poly-α-olefins and cyanoacrylate (CA) instant adhesive.[16–19] These primer effects could be attributed to the interaction between poly-α-olefins and long alkyl chains of primers and the acceleration of curing of CA adhesives. Nevertheless, the mechanism of the primer effect on adhesion has not been revealed in detail because the adhesion phenomena are associated with diverse incidents in the micro- or submicro-scaled interface.[8]

To gain a deeper understanding of the primer effect, we investigated the adhesion strength and surface structure and properties of *it.*PP after casting dimethyloctadecylamine primer. We focused on *it.*PP thin films spin-coated onto silicon wafers as the surface model of adhered specimens. For the evaluation of the surface structure of *it.*PP, small angle incidence X-ray diffraction and X-ray reflection measurements were employed. We investigated the mechanism of the dimethyloctadecylamine primer effect on the enhanced adhesive between *it.*PP and CA adhesives.

Experimental Procedures

1. Preparation of thin films

*It.*PP powder (Noblen HD 100G2, Sumitomo Chemical Co., Ltd.) was Soxhlet-extracted in xylene for 8 h. This extraction removed *atactic* PP and additives. After that, the *it.*PP thin films were prepared from 0.3 wt% tetralin solution by spin-coater at 1,000 rpm for 12 s, then 2,500 rpm for 48 s at 170 °C. 0.1 wt% *N*,*N*-Dimethyl-*n*-octadecylamine in ethanol solution as a primer was coated on the *it.*PP at 800 rpm for 12 s. CA (Loctite401, Henkel Co., Ltd.) was spin-coated on the substrates at 2,500 rpm for 12 s, then 3,500 rpm for 72 s. Under the above conditions, *it.*PP, primer, and *it.*PP + primer thin films with one-, and two-layers were prepared.

2. Small angle incidence X-ray diffraction

The measurements were carried out on SmartLab (Rigaku Co., Ltd., X-ray: CuKα, 40 kV, 30 mA). The incident angle α of the X-ray beam was 0.17°, which was larger than critical angles α_c of *it.*PP (0.146°)[21] and CA (0.156°). Therefore, the penetration depth of the X-ray beam was larger than the thin film thickness, so the structure of the whole film was evaluated. The scintillator detector was scanned perpendicularly to the thin films in the out-of-plane geometry and in the parallel one in the in-plane one. In-plane measurements except for those of only primer in Figure 4 were carried out using a synchrotron beam (beam energy: 10 keV, incidence angle: 0.16°) at SPring-8 BL15XU and BL24XU because their diffraction peaks were undetectable using laboratory apparatus. The profiles measured in SPring-8 were translated to 2θ based on the CuKα wavelength for comparison with the profiles obtained in laboratory measurements.

3. X-ray reflection measurements

The X-ray reflection measurements were also carried out on SmartLab (Rigaku Co., Ltd., X-ray: CuKα, 40 kV, 30 mA). The thickness and roughness of thin films were calculated with software GXRR3 incorporated into the apparatus.

4. Two-dimensional X-ray diffraction with synchrotron radiation at SPring-8

The 2D X-ray diffraction was measured with a synchrotron beam SPring-8 BL15XU and BL24XU. The energy of the X-ray beam was 10 keV. The critical angle α_c for *it.*PP at this beam energy was 0.12°. The incidence angle of the X-ray beam α was 0.14°. The diffraction detector for the 2D X-ray diffraction was Pilutus with a camera length of 435.99 mm.

5. Atomic force microscopy

To investigate the surface roughness, we observed the surface of the thin films in dynamic force mode with E-sweep (SII Nanotechnology Co., Ltd.). Silicon cantilevers with 10 nm of the tip radii were employed.

6. T-peel test

*It.*PP thick films of around 200-μm thickness were prepared by melt-pressing under 6 MPa for 2 min at 200 °C. Amine primer was coated on the *it.*PP. The *it.*PP films with or without amine primer were adhered with CA adhesives. After 24 h, the adhesive strength of their specimens were carried out with autograph AGS-1kND (Shimadzu Co., Ltd.). The test mode was T-peel and the tensile speed was 50 mm/min. The T-peel strength was calculated from the average of five specimens.

7. Dynamic contact angles

The dynamic contact angles of ethylene glycol and diiodomethane were measured at room temperature. The values of the dispersion (γ^d) and polar (γ^p) components of surface free energy for ethylene glycol were 29.3 and 19.0 mJ/m^2 and those of diiodomethane, 48.5 and 2.30 mJ/m^2, respectively.[22] We calculated the surface free energy of the *it*.PP before and after primer treatments from the Young–Owens equation (1) and (2).

$$(1 + \cos \theta) \cdot \gamma_l = 2(\gamma_s^d \cdot \gamma_l^d)^{1/2} + 2(\gamma_s^p \cdot \gamma_l^p)^{1/2} \qquad (1)$$

$$\gamma_s^d + \gamma_s^p = \gamma_s \qquad (2)$$

where θ is an average dynamic contact angle, γ_s and γ_l are the surface free energy of the solid and liquid, and γ^d and γ^p are dispersion and polar components, respectively.[22]

Results and discussion

The structures of *it*.PP thin film (Figure 1a) and *it*.PP thick film (Figure S1 in supplementary information) without both primers were evaluated by X-ray diffraction. Judging from the profiles, the observed diffraction peaks could be indexed with the most conventional α-form.[21,23] The *it*.PP thick films, which were prepared by melt pressing, showed random crystallite orientation. In contrast, the diffraction profiles of *it*.PP thin films with in-plane and out-of-plane geometry were distinct from that of the thick film, and those in-plane and out-of-plane profiles were quite different. In the out-of-plane geometry, the major diffraction peak at 2θ = 13° was assigned to the (110) plane of the α-form *it*.PP, while the profiles with in-plane geometry provided the three diffraction peaks at 2θ = 13°, 16° and 19° from (110), (040) and (130) planes, respectively. These results revealed that the crystallites in the *it*.PP thin film were oriented as schematically shown in Figure 2. The a* axis was standing perpendicular to the substrates and 3/1 helix of the *it*.PP molecule lay parallel to the silicon wafer substrate.[21,23] The X-ray diffraction profiles of the *it*.PP thin film after application of the amine primer are shown in Figure 1b. In the out-of-plane profile, no difference was observed from that without primer, whereas the diffraction peak at 2θ = 21° emerged in the in-plane profiles. To allow detailed observation of the crystallite orientation, two-dimensional diffraction images were measured as shown in Figure 3. In the 2D image of *it*.PP thin films without primer, the 110 diffraction was clearly observed in the out-of-plane direction, then the diffraction from the (111) plane was observed in the direction tilted by 45° from the in-plane axis. These results support the crystallite orientation of *it*.PP thin film as shown in Figure 2. On the contrary, in the 2D image of *it*.PP thin film with primer, the diffraction intensity at 2θ = 21°on the in-plane axis increased relative to those of the other diffraction on the in-plane axis.

(Figure 1.)

(Figure 2.)

(Figure 3.)

To investigate the appearance of the diffraction peak at 2θ = 21° in the in-plane measurements, the primer thin films were only applied to the silicon wafer substrates. The X-ray diffraction profiles in the in-plane geometry are shown in Figure 4. After spin-coating the primer on the substrates, the diffraction peaks appeared at 2θ = 21°. This diffraction angle corresponded to that appearing on the *it.*PP thin films with primers (Figure 1b). Moreover, the longer open time and exposure time to ambient atmosphere after the primer treatment led to a stronger diffraction peak. In contrast, no diffraction peak was observed at 2θ = 21° in the out-of-plane geometry. These results indicate that the long alkyl chains of the primer might stand perpendicular to the silicon wafer substrates as well as on the *it.*PP thin films.

(Figure 4.)

Table 1 shows the thickness and surface roughness of *it.*PP before and after primer treatment measured with X-ray reflectivity (XRR) and atomic force microscopy (AFM). XRR profiles and AFM topography are shown in Figure S2 and S3 of supporting information, respectively. The calculated roughness values from the XRR profiles and AFM topography coincided with each other. From the fitting of the XRR profiles, their parameters before primer treatment were 35.6 nm and 2.5 nm, while those after treatment were increased. Thus, the primer layers might be formed within the primer through swelling of the surface of the *it.*PP thin films.

(Table1)

For the examination of the primer effect on adhesive strength, the T-peel tests were performed. In the preparation of these specimens, an open time of 5h was employed.

The adhesive strength without primer treatments was 1.8 N/cm and peeling occurred at the interface between the CA adhesives and the *it.*PP. The adhesive strength of specimens after primer treatments reached 30 N/cm and the *it.*PP substrates were fractured. A dominant primer effect was observed. The amine primer accelerated the CA curing reaction, and then enhanced the interaction between *it.*PP and CA adhesives.

For a deep insight into the primer effect, we performed T-peel tests, together with measurements of contact angles and in-plane small angle incidence X-ray diffraction with various open times. Figure 5 shows the effect of open time on T-peel strength and surface free energy, γ. T-peel strength increased with open time after primer treatments. T-peel strength peaked at 5 h of open time, after which the adhesive strength decreased again. The γ value was increased after primer treatment relative to the non-treated surface. That is, the surface hydrophilicity increased with primer treatment. Then, with a longer open time, the γ value increased within 5 h and then decreased. The in-plane small angle incidence X-ray diffraction profiles with various opens time are shown in Figure 6. After primer treatment, the intensity of the diffraction peaks at 21° increased within 5 h, and then decreased after 9 h of open time. Accordingly, the dependences of the adhesive strength, surface free energy and the structure of the amine primer on the *it.*PP surface on open time were synchronized with one another.

(Figure 5.)

(Figure 6.)

Therefore, the high alignment of primer molecules at the interface is considered to effectively enhance the adhesion between CA and *it.*PP.

Conclusions

We summarized the effect of dimethyloctadecylamine primer on the adhesion strength between *it*.PP and CA adhesives. The structure of *it*.PP in thin film was oriented on the silicon wafer. The main chains were aligned in the parallel direction to the substrate surface. The amine primer assisted the adhesion strength between *it*.PP and CA adhesives. This enhancement mechanism is considered to be attributed to the formation of assembled primer structure on *it*.PP. The intensity of peaks originating from assembled primer in X-ray diffraction measurements affected the surface free energy of *it*.PP and the adhesion strength of the *it*.PP/CA/*it*.PP specimen. Their parameters simultaneously depended on the open time. Accordingly, the formation of the primer layer after application to *it*.PP substrates achieved higher adhesive strength.

ASSOCIATED CONTENT

Supplementary Data.

This material is available free of charge via the Internet at http://

AUTHOR INFORMATION

Corresponding Author

*(T.N.) E-mail: tnishino@kobe-u.ac.jp

Notes

The authors declare no competing financial interest.

ACKNOWLEDGEMENT

The synchrotron radiation experiments were performed at the BL15XU, BL24XU of SPring-8 with the approval of the National Institute for Materials Science (NIMS) and the Japan Synchrotron Radiation Research Institute (JASRI) (Proposal No. 2011B3255, 2012A4803, 2012B4803).

REFERENCES

[1] Galli P, Vecellio G. Polyolefins: The most promising large-volume materials for the 21st century. J Polym Sci Part A Polym Chem 2004;42:396–415. doi:10.1002/pola.10804.

[2] Karian HG. Handbook of Polypropylene and Polypropylene Composites: Second Edition, Revised and Expanded. Marcel Dekker, Inc.; 2003.

[3] Paul DR, Robeson LM. Polymer nanotechnology: Nanocomposites. Polymer 2008;49:3187–204. doi:http://dx.doi.org/10.1016/j.polymer.2008.04.017.

[4] Tjong SC. Structural and mechanical properties of polymer nanocomposites. Mater Sci Eng R Reports 2006;53:73–197. doi:http://dx.doi.org/10.1016/j.mser.2006.06.001.

[5] Hussain F, Hojjati M, Okamoto M, Gorga RE. Review article: Polymer-matrix Nanocomposites, Processing, Manufacturing, and Application: An Overview. J Compos Mater 2006;40:1511–75. doi:10.1177/0021998306067321.

[6] Coates GW. Precise Control of Polyolefin Stereochemistry Using Single-Site Metal Catalysts. Chem Rev 2000;100:1223–52. doi:10.1021/cr990286u.

[7] Coates GW, Hustad PD, Reinartz S. Catalysts for the Living Insertion Polymerization of Alkenes: Access to New Polyolefin Architectures Using Ziegler–Natta Chemistry. Angew Chemie Int Ed 2002;41:2236–57. doi:10.1002/1521-3773(20020703)41:13<2236::AID-ANIE2236>3.0.CO;2-3.

[8] Awaja F, Gilbert M, Kelly G, Fox B, Pigram PJ. Adhesion of polymers. Prog Polym Sci 2009;34:948–68. doi:http://dx.doi.org/10.1016/j.progpolymsci.2009.04.007.

[9] Liston EM, Martinu L, Wertheimer MR. Plasma surface modification of polymers for improved adhesion: a critical review. J Adhes Sci Technol 1993;7:1091–127. doi:10.1163/156856193X00600.

[10] Encinas N, Oakley BR, Belcher MA, Blohowiak KY, Dillingham RG, Abenojar J, et al. Surface modification of aircraft used composites for adhesive bonding. Int J Adhes Adhes 2014;50:157–63. doi:http://dx.doi.org/10.1016/j.ijadhadh.2014.01.004.

[11] Baldan A. Adhesively-bonded joints and repairs in metallic alloys, polymers and composite materials: Adhesives, adhesion theories and surface pretreatment. J Mater Sci 2004;39:1–49. doi:10.1023/B:JMSC.0000007726.58758.e4.

[12] Yang Q, Xu Z-K, Dai Z-W, Wang J-L, Ulbricht M. Surface Modification of Polypropylene Microporous Membranes with a Novel Glycopolymer. Chem Mater 2005;17:3050–8. doi:10.1021/cm048012x.

[13] Chan C-M, Ko T-M, Hiraoka H. Polymer surface modification by plasmas and photons. Surf Sci Rep 1996;24:1–54. doi:http://dx.doi.org/10.1016/0167-5729(96)80003-3.

[14] ten Cate AT, Reinders SAF, Turkenburg DH, Bruin A, D'Souza F, Donnelly GT, et al. High density hydrophilic and hydrophobic brush coatings using a polymeric primer layer. Prog Org Coatings 2009;64:221–4. doi:http://dx.doi.org/10.1016/j.porgcoat.2008.08.029.

[15] Gerenser LJ. XPS studies of in situ plasma-modified polymer surfaces. J Adhes Sci Technol 1993;7:1019–40. doi:10.1163/156856193X00556.

[16] Goel V, Beginn U, Mourran A, Möller M. "Quat-Primer" Polymers Bearing Cationic and Reactive Groups: Synthesis, Characterization, and Application. Macromolecules 2008;41:8187–97. doi:10.1021/ma801064e.

[17] Klemarczyk P. The isolation of a zwitterionic initiating species for ethyl cyanoacrylate (ECA) polymerization and the identification of the reaction products between 1°, 2°, and 3° amines with ECA. Polymer 2001;42:2837–48. doi:http://dx.doi.org/10.1016/S0032-3861(00)00618-2.

[18] Yang J, Garton A. Primers for adhesive bonding to polyolefins. J Appl Polym Sci 1993;48:359–70. doi:10.1002/app.1993.070480220.

[19] Okamoto Y, Klemarczyk PT. Primers for Bonding Polyolefin Substrates with Alkyl Cyanoacrylate Adhesive. J Adhes 1993;40:81–91. doi:10.1080/00218469308031275.

[20] Kimura K. Adhesives for Polyolefine Resins. J Adhes Soc Japan Adhes 1987;23:443–8.

[21] Nishino T, Matsumoto T, Nakamae K. Surface structure of isotactic polypropylene by X-ray diffraction. Polym Eng Sci 2000;40:336 –43. doi:10.1002/pen.11167.

[22] Owens DK, Wendt RC. Estimation of the surface free energy of polymers. J Appl Polym Sci 1969;13:1741–7. doi:10.1002/app.1969.070130815.

[23] Natta G, Corradini P. Structure and properties of isotactic polypropylene. Nuovo Cim 1960;15:40–51. doi:10.1007/BF02731859.

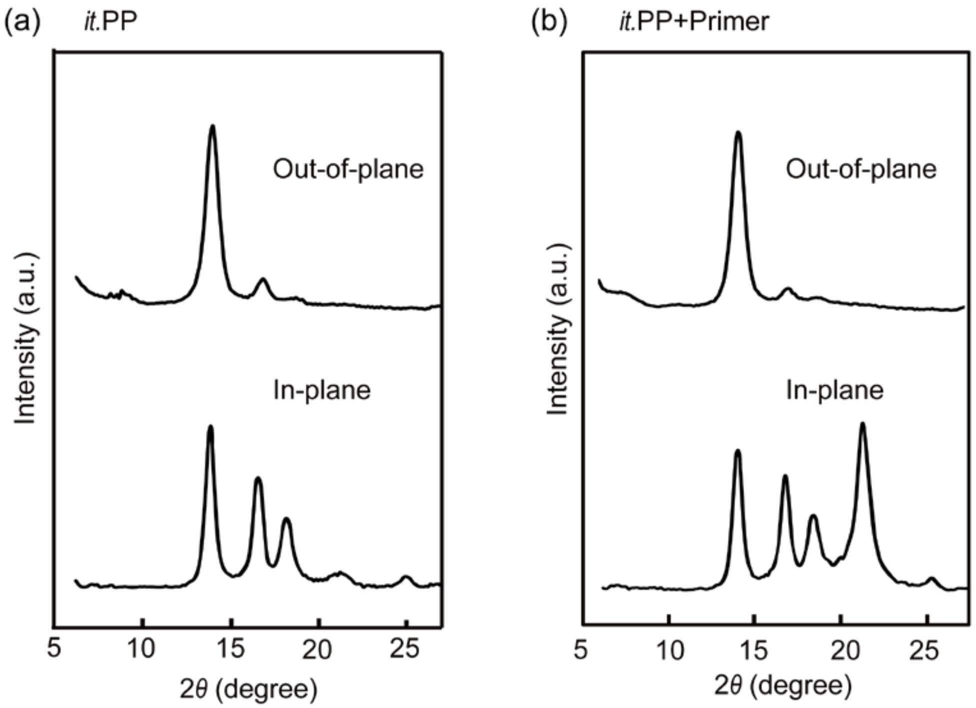

Figure 1. Small angle incidence X-ray diffraction profiles of *it.*PP thin films (a) before and (b) after application of the primer with out-of-plane and in-plane geometries.

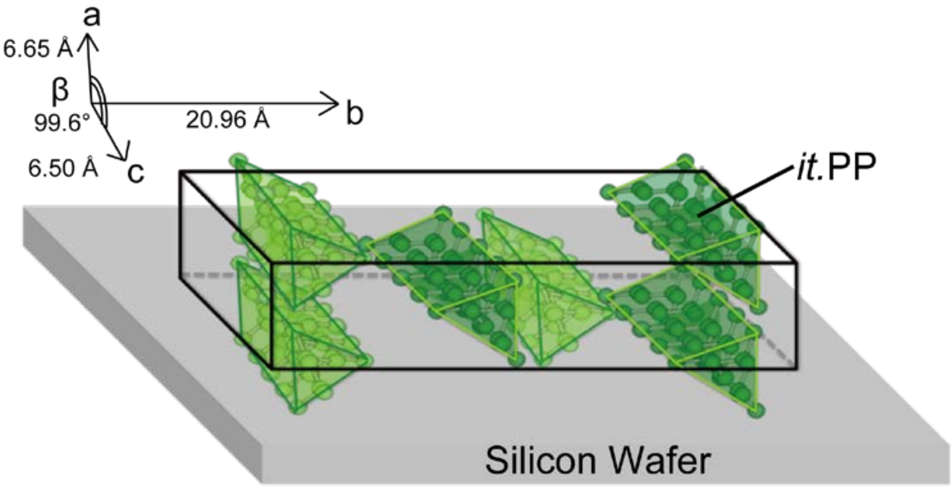

Figure 2. Schematic representation of the crystallite orientation of *it*.PP in the thin film spin-coated onto a silicon wafer.

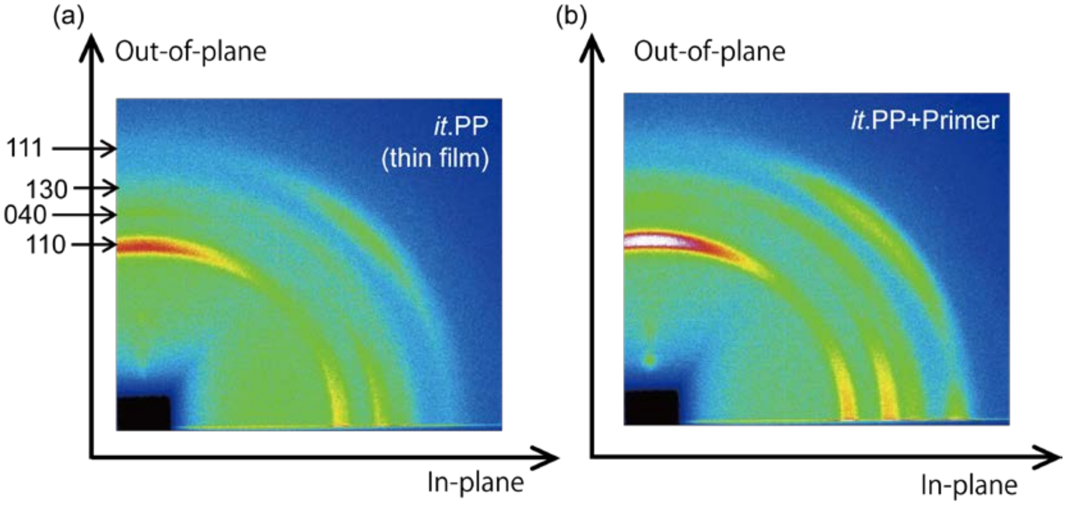

Figure 3. 2D small angle incidence of X-ray diffraction profiles of *it*.PP thin films (a) before and (b) after application of primer.

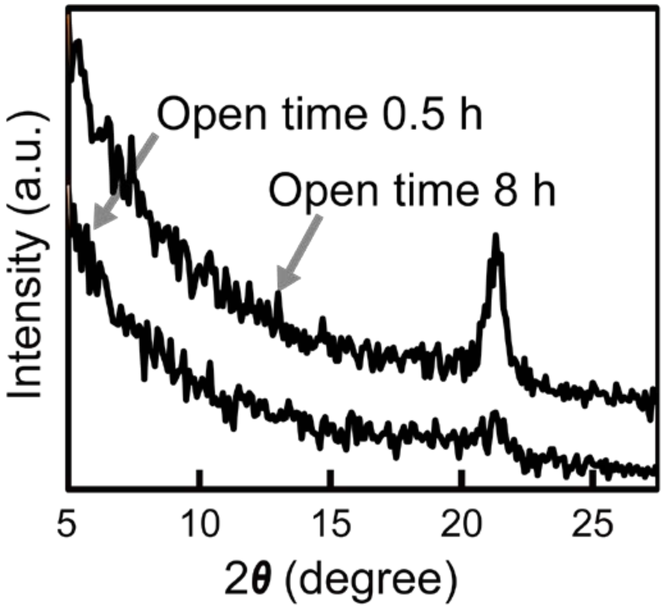

Figure 4. Small angle incidence X-ray diffraction profiles of amine primer 0.5 h and 8 h after spin-coating onto the silicon wafers with in-plane geometry.

Table 1. Thickness and roughness of *it*.PP thin films before and after application of primer.

	Thickness (nm)	Roughness (nm)
it.PP	35.6[a]	2.5[a] (2.4[b])
it.PP + primer	40.1[a]	4.0[a] (4.4[b])

[a] Calculated from X-ray reflection profiles. [b] Calculated from AFM geometries.

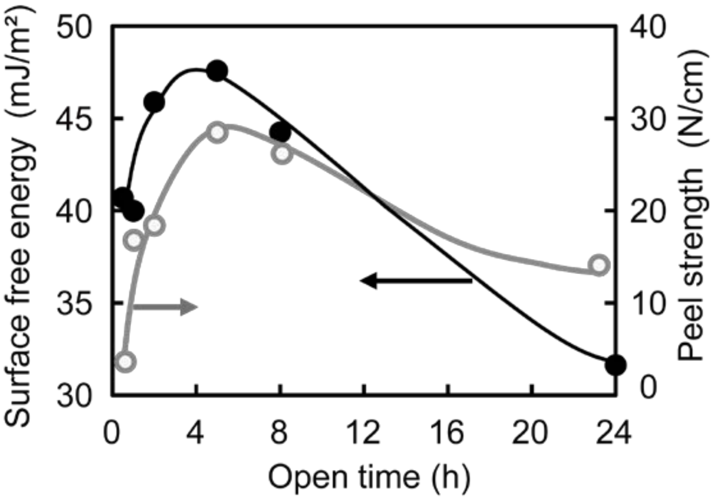

Figure 5. Relationship between surface free energy of *it*.PP thin film, T-peel strength between *it*.PP/CA and the open time after application of the primer.

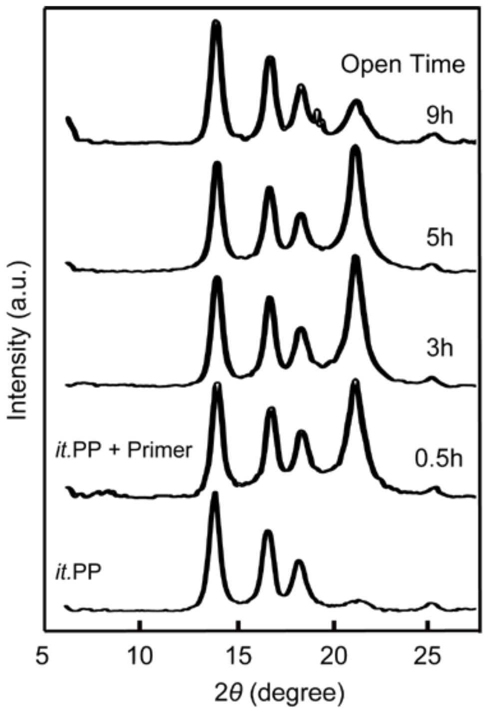

Figure 6. Small angle incidence X-ray diffraction profiles of *it*.PP thin films 0, 0.5, 3 and 9 h after application of the primer with in-plane geometry.

TOC

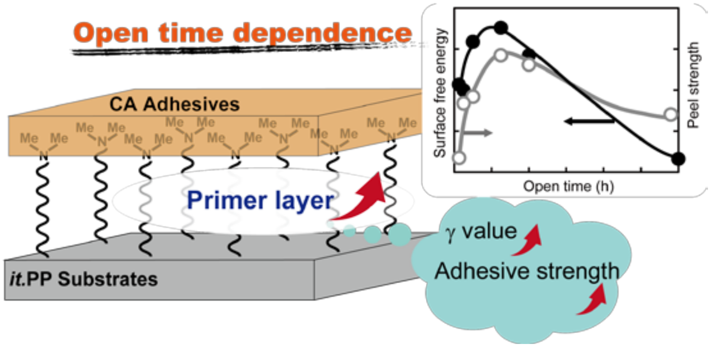
Open time dependence
CA Adhesives
Me Me N
Primer layer
it.PP Substrates
γ value
Adhesive strength
Surface free energy
Peel strength
Open time (h)

Electronic Supplementary Material

Adhesion Enhancement by Amine Primer Applying on Isotactic Polypropylene and Open Time Dependence

Megumi Komada[a], *Yuta Nakanishi*[a], *Takuya Matsumoto*[a], *Masaru Kotera*[a], *Chizuru Hongo*[a], *and Takashi Nishino**[a]

[a] Department of Chemical Science and Engineering, Graduate School of Engineering, Kobe University Rokko, Nada, Kobe, 657-8501, Japan

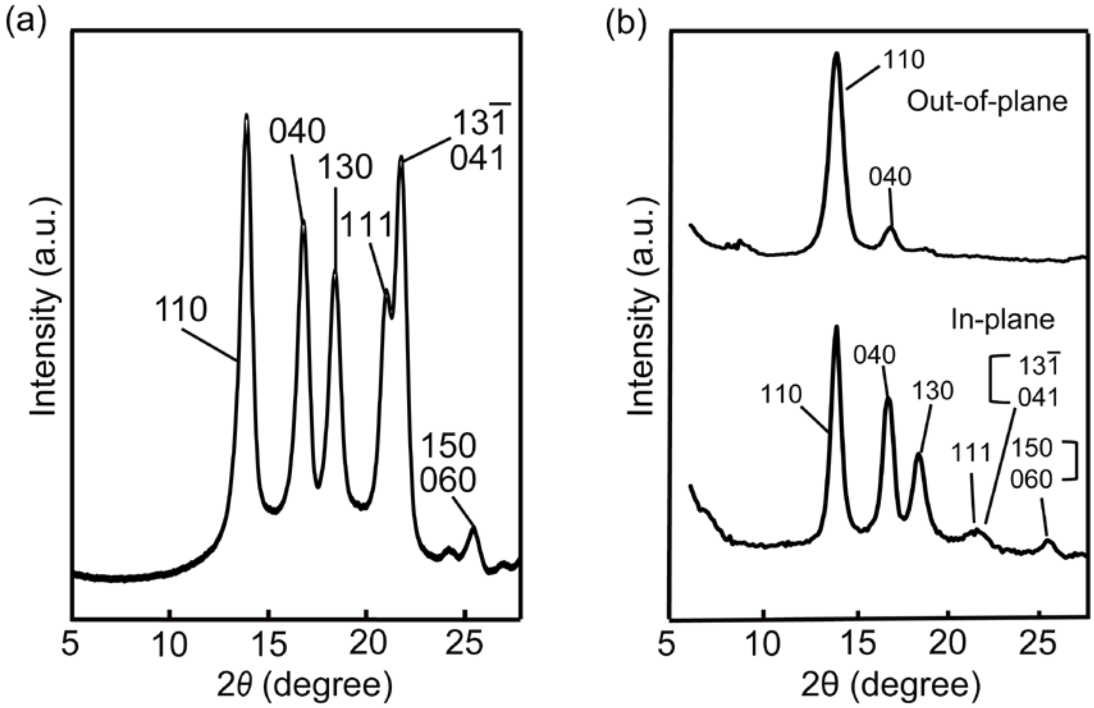

Figure S1. (a) X-ray diffraction profile of *it*.PP thick film and (b) small angle incidence X-ray diffraction profile of *it*.PP thin film.

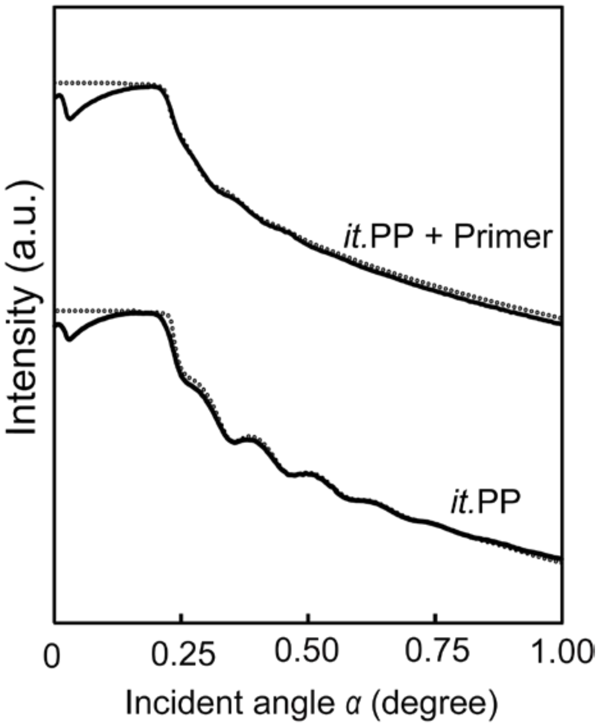

Figure S2. X-ray reflective profiles of *it.*PP and *it.*PP +primer.

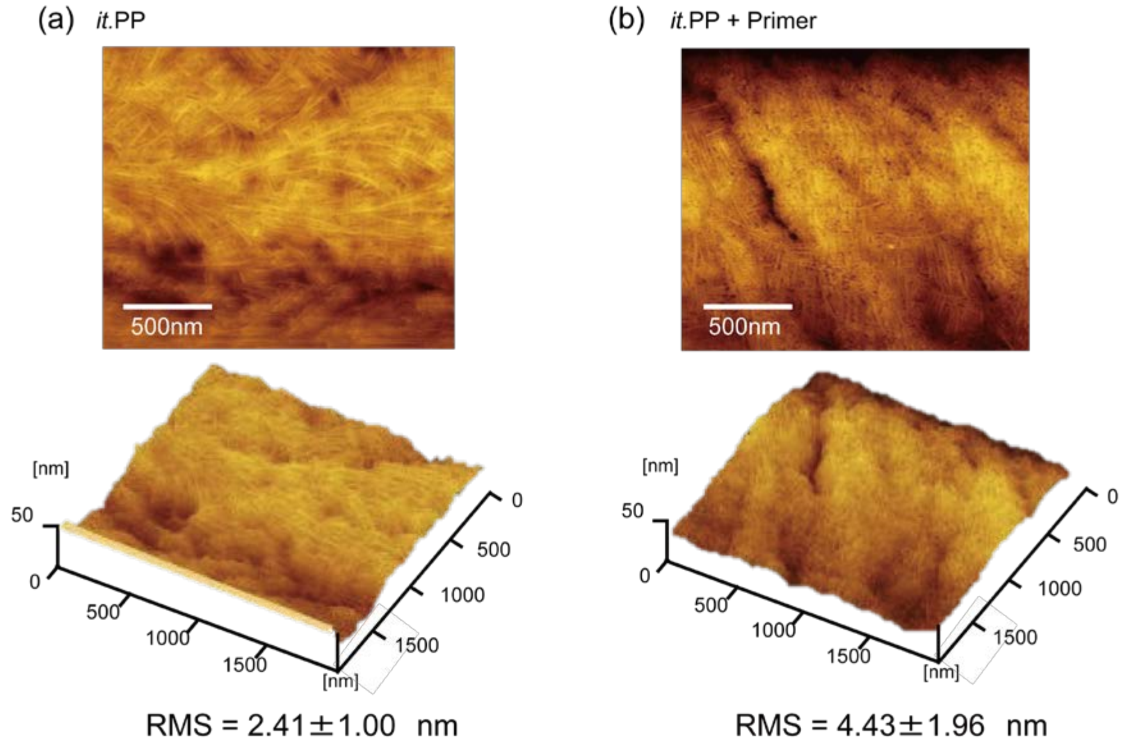

Figure S3. AFM height images of (a) *it.*PP and (b) *it.*PP +primer.